J Mater Sci (2009) 44:5595–5601
DOI 10.1007/s10853-009-3787-y

Electromigration behaviors in Sb particle-reinforced composite eutectic SnAgCu solder joints

Fu Guo · Guangchen Xu · Hongwen He

Received: 13 April 2009 / Accepted: 30 July 2009 / Published online: 8 August 2009
© Springer Science+Business Media, LLC 2009

Abstract Due to the limited capacity of solder joints in microprocessors for the higher current density (usually 10^3–10^4 A/cm^2), electromigration (EM), known as the mass movement resulting from imposition of high current density, has gained extensive attention during the last decades, specifically, the EM-induced damages in the eutectic 95.5Sn–3.8Ag–0.9Cu (e-SAC) that were heavily used in the electronic packaging industry. In order to conquer the instable physical properties of e-SAC in the severe service environment, composite approach was developed. One of the promising ways was intentionally incorporated metal-particles reinforcements. In this study, the e-SAC with 1 wt% Sb particles additive was investigated under the current density of 10^4 A/cm^2 and 120 °C the ambient temperature. Unlike the non-composite solders that had obvious formation of hillock and valley at the anode side and cathode side, respectively. The crack initiated at the edge of the cathode interface and propagated to the center in the Sb particle-reinforced composite solder. The Sn–Sb phase, formed near the cathode interface after the first-reflow, blocked the movement of metal atoms/ions, but then induced the current crowding. In addition, synergistic influence of the compressive and tensile stress caused the fracturing of the Sn–Sb phase in the solder matrix due to its brittleness and immobility.

F. Guo · G. Xu · H. He
College of Materials Science and Engineering, Beijing University of Technology, Beijing, China

G. Xu (✉)
Department of Chemical Engineering and Materials Science, Michigan State University, East Lansing, MI, USA
e-mail: gcxu@msu.edu

Introduction

During the past 10 years of studies on the reliability issues of lead-free solder joints, people realized the properties of the first generation lead-free solders, such as eutectic 58Bi–42Sn, 96.5Sn–3.5Ag, and 95.5Sn–3.8Ag–0.7Cu, were less satisfied to meet the need of high-performance electronic products, specifically servers, storage and storage array systems, network infrastructure equipment, and network management for telecommunication equipment [1]. Accordingly, researchers proposed several methods to improve the properties of the first generation lead-free solders. Ex-situ composite solders (addition of the micro-sized particles of Cu, Ag, and Ni) longer extended the creep-to-failure of lead-free solder joints [2, 3]; trace rare-earth doping could also stabilize the intermetallic compounds (IMCs) at the interface during the isothermal aging [4]. These newly developed lead-free solders are the prominent ones to substitute the first generation ones. However, with the shrinking size of the electronic products, every single solder joint in components should carry more electrical current than before, usually 10^3–10^4 A/cm^2. Under this level, electromigration (EM) could break the circuit due to the mass depletion at the cathode side [5–7]. In order to solve this threat to the electronic solder joints, lots of works have been accomplished. According to literatures [8–10], Tu et al. employed thick Cu UBM (under bump metallization), which enabled a redistribution of current, so the current density in the solder bump would be much closer to the average value. Chen et al. doped 1 wt% Cu into the eutectic SnBi solder, more Bi accumulation and more severe solder depletion were observed in the Cu-doped solder stripe. On the other hand, they also doped 0.5 wt% Ag into the eutectic SnBi solder, and the plate-like Ag_3Sn, formed after doping into the solder, and intercepted the Bi migration from the cathode side

to the anode side which made a divergence of atomic flux to take place. It is noteworthy that metal elements in addition to lead-free solders may enhance the EM damage, or retard it. Accordingly, it is necessary to re-analyze on this issue. Based on our current knowledge, there are few reports and studies concerning Sb particle-reinforced composite solder. Adding Sb can improve the wettability and mechanical properties of the lead-free solder. But the microstructure evolution of solder joints was not well understood during the current stressing. Thus, the aim of this study is to investigate the effect of Sb particle on the EM behaviors of the eutectic 95.5Sn–3.8Ag–0.7Cu solder (e-SAC), and evaluates the corresponding failure mechanism.

Experimental procedures

The composite solder was prepared by mechanically mixing the e-SAC solder paste with 6 μm sizes of 1 wt% Sb reinforcement particles. To achieve the uniform distribution of the reinforcement particles in the paste matrix, at least 15 min was used for mixing. The solder joints with one-dimensional structure were fabricated to conduct EM study. Figure 1 is the schematic drawing of the set-up for soldering. Two copper wires with 500 μm diameter were first placed into a soldering die with U-grooves, one of which was connected to the X-Y-Z translating stage, and then a 5 mg prepared solder paste was placed into the gap between two copper wires. Finally, the die with specimen was entirely heated up and then cooled down to the room temperature rapidly by a fan. After the solder joints were fabricated, it then cold mounted in the epoxy resin, in order to reach the current density to a high level (10^4 A/cm^2), half dimension of the specimen was ground and polished off to reach a dimension with a cross-sectional area of 1×10^{-3} cm^2, as illustrated in Fig. 2. After that the specimen was put into an

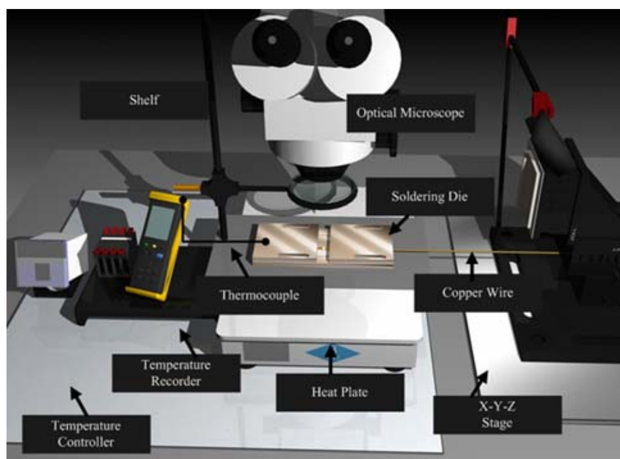

Fig. 1 Schematic drawing of the set-up for the soldering

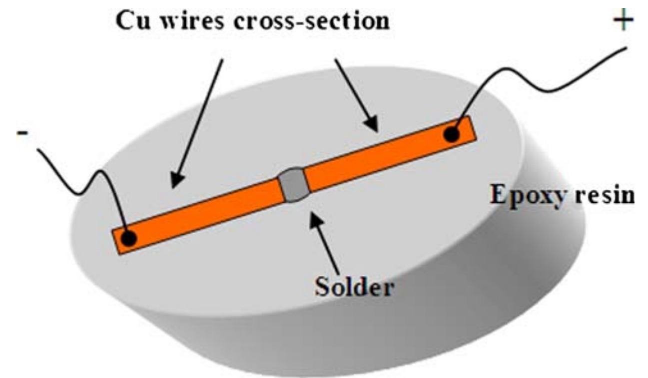

Fig. 2 Schematic drawing of the specimen during the current stressing

oven where temperature was set to 120 °C, a current of 10 A was continuously applied to the specimen; the current density of which being 10^4 A/cm^2. A detailed procedure can be found in our pervious publications [11–13]. For observation of the microstructure evolution in the solder joints during the EM test, technique of scanning electron microscope (SEM) was used. An energy-dispersive X-ray (EDX) spectrum was used to help analyze the compositions of the detected regions.

Results and discussion

Initial state (as-reflowed microstructure)

It has been reported that the Sn–3.5Ag–0.7Cu–1%Sb solder may consist of several phases, i.e., the primary Sn-rich phase [Sn(Sb), Sb ≤ V 7 wt%], the Ag_3Sn phase, ε-Ag_3(Sn, Sb) compound, Cu_6Sn_5 phase, and Cu_3Sn phase [14]. EDX analysis of Fig. 3 indicates that the particles in the solder matrix consisting of Sn and Sb. What is more, Sn and Sb share the same spectrum, so it is difficult to illustrate the exact composition rate from the EDX results. The results of the point detection are list in Table 1. Sn accounts for most constitution in the Sn–Sb particles due to the trace Sb additive in the solder matrix. According to the Sn–Sb phase diagram, as illustrated in Fig. 4, the abscissa represents the composition of the alloy in weight percent (top) and atom percent (bottom) of Sb, some phase boundary lines near the bottom of Fig. 4 are dashed to indicate that their positions have not been exactly determined. The reason for this is that at low temperatures, diffusion rates are very slow and inordinately long times are required for the attainment of equilibrium. Figure 5 shows the element mapping on a square area, Cu was seldom detected, but both Sn and Sb appeared on the full area, specifically the Ag particles were found on the surface of the Sn–Sb particles. Figure 6 is the line scanning of elements at the interface, and Sb was not

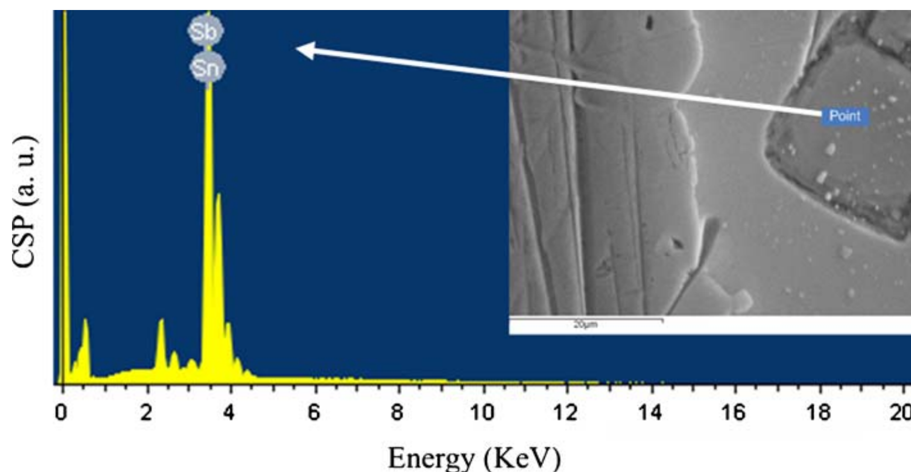

Fig. 3 Energy spectrum of Sn and Sb by the point detection of EDX

Table 1 Results of the point detection on the Sn–Sb particle

Element	Weight (%)	Atomic (%)
Sn L	97.79	97.85
Sb L	2.21	2.15
Total	100	100

found at the interface, indicting Sb only reacted with Sn to form the particles in the solder matrix.

Figure 7a is the optical micrograph (OM) which shows the as-reflowed microstructure of e-SAC with 1 wt% Sb particles addition. Due to the enhancement of contrast in OM, the dark region is the formed Sn–Sb particles in the solder matrix, the gray region consists two phases which are Sn and IMCs. By introducing the professional software ImageJ^{TM}, a public domain Java-based image processing program, quantification of the Sn–Sb particles becomes possible. Before counting and measuring objects in the microstructure, the particle analyzer should be configured. By entering a single value in 5 μm^2, the particles smaller than that value were ignored. Accordingly, the profiles of the Sn–Sb particles were obtained by ImageJ^{TM}, as shown in Fig. 7b. A total of 179 particles were detected out. The average size of the Sn–Sb particles was calculated to be 68.32 μm^2, and the area fraction of the Sn–Sb particles was calculated to be 11.14%.

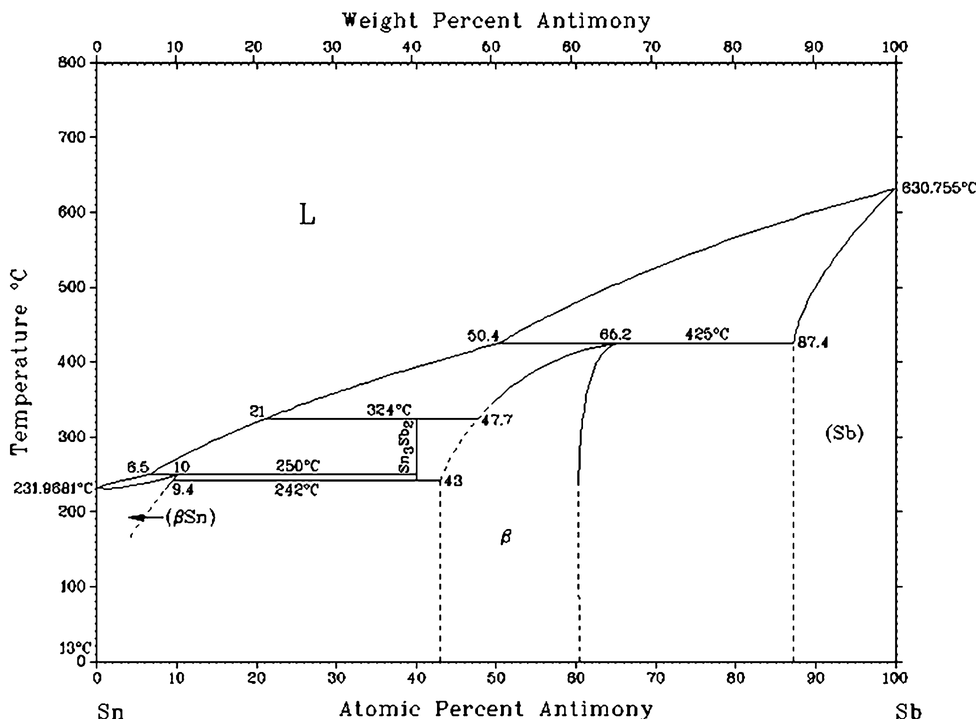

Fig. 4 The Sn–Sb phase diagram

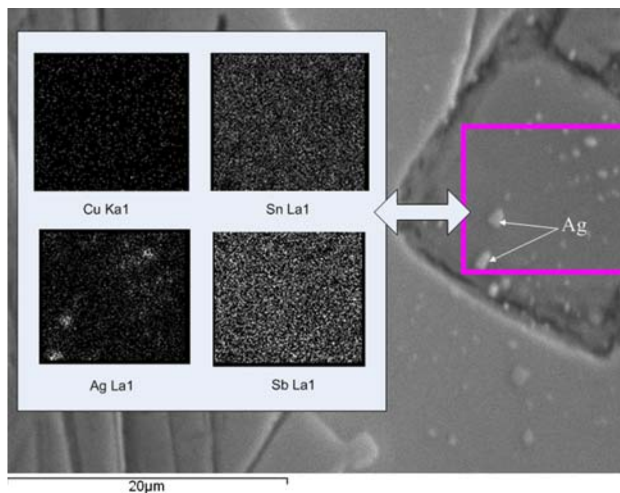

Fig. 5 Elements mapping of Cu, Sn, Ag, and Sb on the Sn–Sb particle in solder matrix

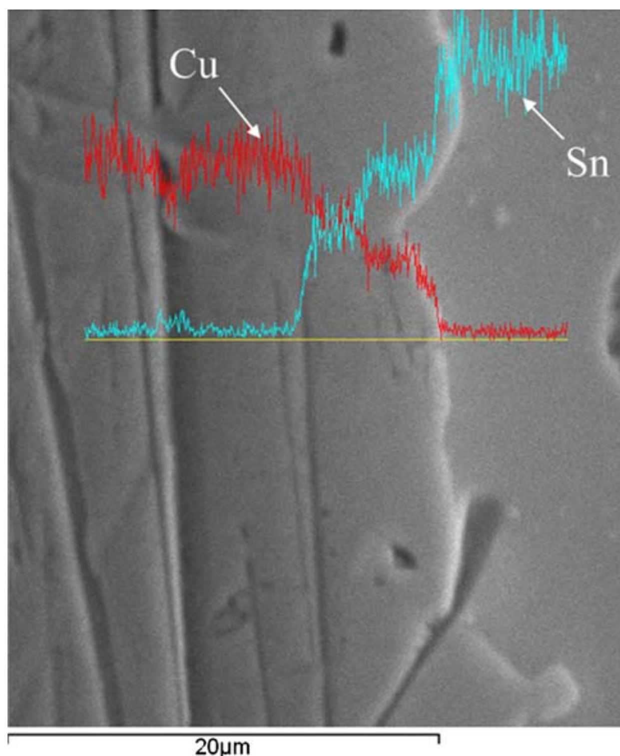

Fig. 6 Linear scanning of the EDX at the interface between Cu substrate and solder matrix

Microstructural evolution of the Sn–Sb particles in solder matrix

Figure 8 shows a set of microstructural evolution of the Sn–Sb particles during current stressing. As shown in Fig. 8a, the Sn–Sb particles were embedded in the bulk solder after the first-reflow. However, after 240 h of current stressing, the decohesion occurred between the Sn–Sb particles and the solder matrix, as shown in Fig. 8b, demonstrating the bonding strength of the Sn–Sb particles with the surrounding solder matrix was weak. In addition, the crack went through the Sn–Sb particles showed its brittleness feature, as shown in Fig. 8c. It is important to note that the size of the Sn–Sb particles remained during the current stressing, illustrating the Sb could not react with Sn further. Therefore, the cracks in the Sn–Sb particles were not contributed to the chemical reactions, but the mechanical stress induced by the movement of metal atoms/ions in the bulk solder.

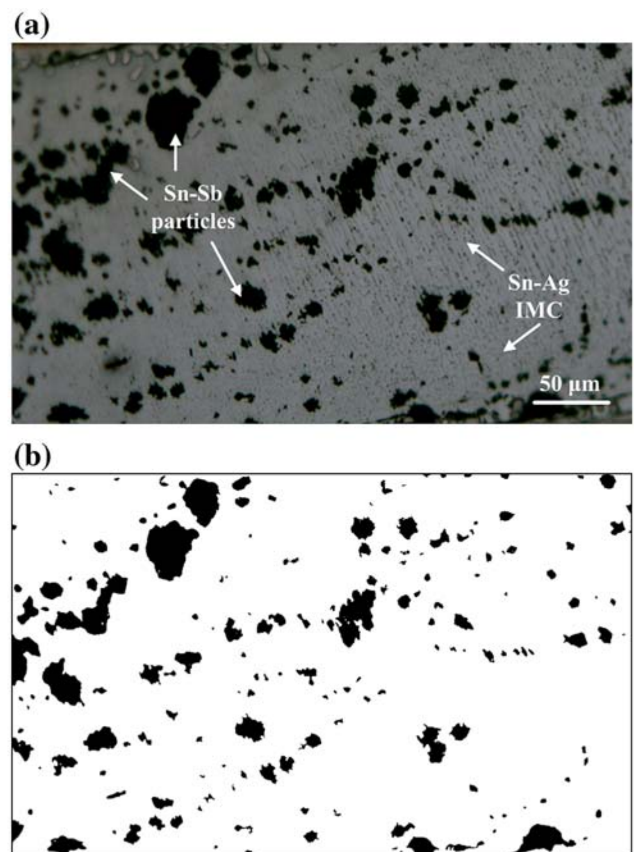

Fig. 7 **a** OM image of the cross-sectional solder matrix, **b** profile of the Sn–Sb particles obtained by the ImageJ™

Microstructural evolution at the interfaces

In order to identify the effect of EM behaviors on the Sb-particles reinforced composite solder, non-composite one was employed for the comparative study. As shown in Fig. 9a, after 240 h of the current stressing, the solder bulged at the anode side due to the accumulation of the solder, and the valley formed at the cathode side due to the depletion of the solder. In addition, the Sn–Cu IMCs at the anode interface extruded as well, because the metal

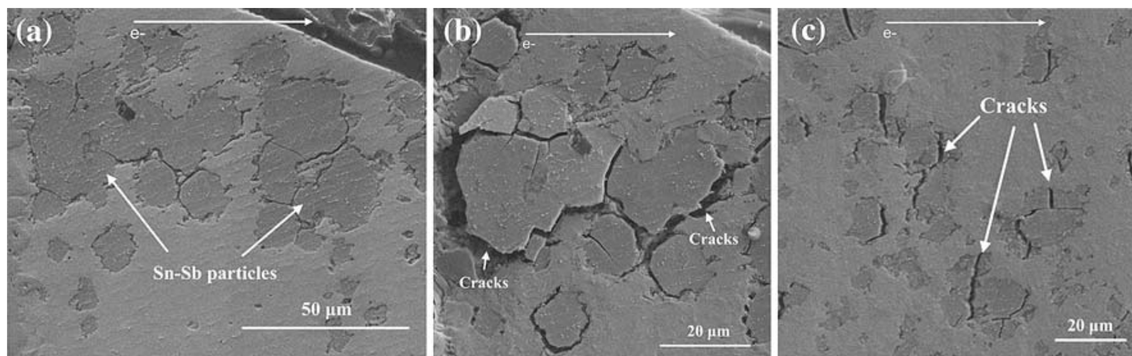

Fig. 8 **a** The microstructure of Sn–Sb particles in the solder matrix without the current stressing; **b** the microstructure of Sn–Sb particles in the solder matrix after 200 h of the current stressing; **c** the cracks went through the Sn–Sb particles in the solder matrix during the current stressing

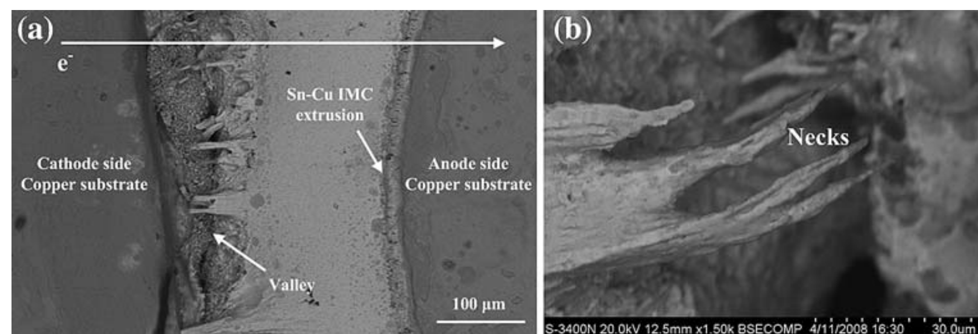

Fig. 9 **a** The microstructure of the e-SAC solder joints after 240 h of the current stressing; **b** formation of the necks near the cathode side

atoms/ions in solder matrix cannot diffuse into the Cu substrate. Due to the ductility of solder alloy by nature [15, 16], there was more plastic deformation at the increased ambient temperature. At the maximum tensile stress, some small constrictions or necks began to form at some point, elongation direction became aligned parallel to the direction of electron wind flow, and all subsequent deformation was confined at these necks, as indicated in Fig. 9b, and fracture (formation of the valley) ultimately occurred at these necks.

Unlike the EM behaviors of e-SAC solder, we did not find the valley formation in the composite one, instead of that, a pancake crack was observed. As shown in Fig. 10a, before the current stressing, the solder matrix was well bonded with the Cu substrate through IMCs layer at the cathode interface. However, after 240 h of current stressing, the crack initiated and propagated from the edge to the center at the cathode interface. As shown in Fig. 10c, which is the enlarged image form of Fig. 10b, the solder matrix divorced from the IMCs layer, demonstrating that the interfacial bonding strength between the Cu substrate and the IMCs layer was weaker than that between the solder matrix and the IMCs layer.

In addition, the deformations observed at the anode side are presented in Fig. 11. After 240 h of the current stressing, the most intense plastic deformation occurred near the solder/Cu interface at the anode side. The mass flow toward the direction of electrons caused the accumulation of metal atoms/ions at the anode side. The most noticeable features are an increase in the surface upheaval due to the protruding solder and Sn–Cu IMCs.

Chen et al. [17] employed the 3D finite element method to simulate the current and temperature redistributions due to the formation and propagation of a pancake-shape void in solder joints during EM. It is proposed that current redistribution is the main reason accounting for crack formation and propagation, especially the propagation into the low current density region below the contact passivation. However, this current redistribution was mainly contributed by the unique geometry of flip chip solder joints (line-to-bump). The current density at the entrance corner is approximately one order of magnitude higher than the average current density in the bump, which is defined as the current crowding region. In our EM test, the one-dimensional structure guaranteed the straight movement of the electrons from the cathode side to the anode side, which eliminated the current crowding region. Although the electrons moved straight, the pancake-crack could form at the cathode interface. As mentioned above, the Sn and Sb could not react further during the current stressing. Thus, the Sn–Sb particles could redistribute the current density. The metal atoms/ions could be propelled by the electron wind force under high current density, but the movement of the metal atoms/ions was blocked after they impinged on

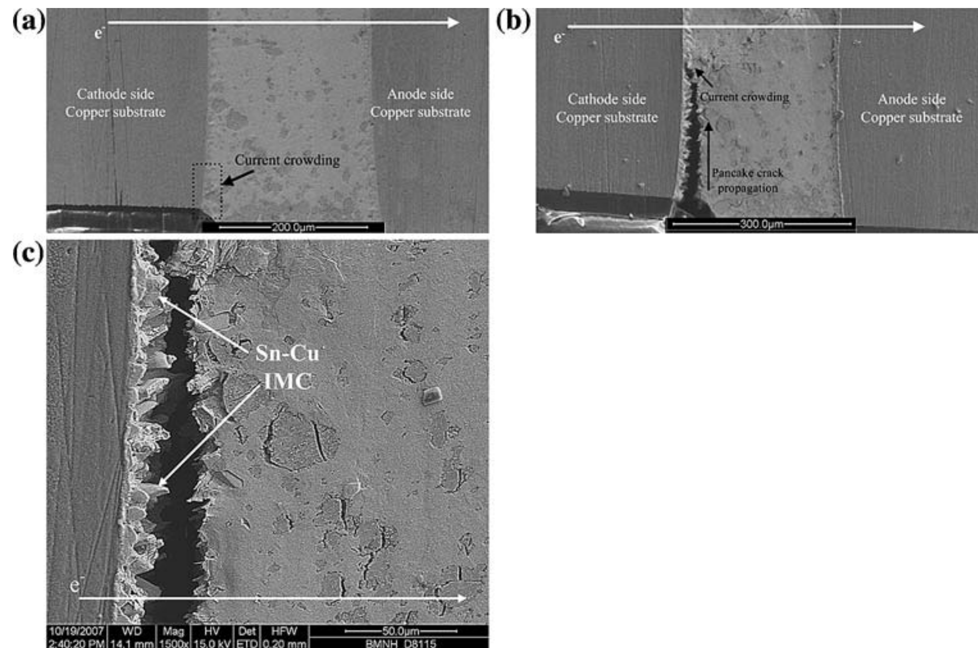

Fig. 10 Formation and propagation of the pancake void at the cathode side **a** without current stressing; **b** current stressing after 240 h; **c** void formed between the solder matrix and the Sn–Cu IMCs

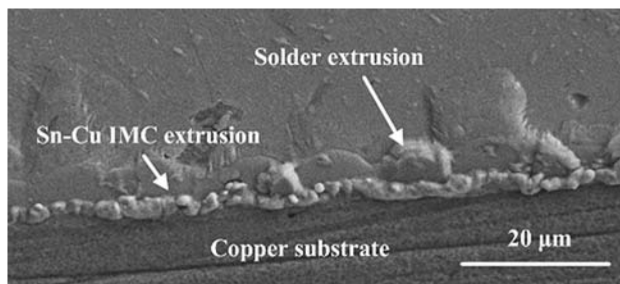

Fig. 11 Extrusion of solders and Sn–Cu IMCs at the anode side

the Sn–Sb particles. Accordingly, the generated-stress around the Sn–Sb particles made them rupture. Therefore, the local current density was much higher than other area, and induced the melting of solder at the edge. Under the tensile stress, the crack propagated from the edge to the center at the cathode interface.

Conclusions

Solder joints with one-dimensional structure were developed which eliminated the effects of current crowding and thermomigration in flip chip bumps. A total of 1 wt% Sb particles was added into the e-SAC solder. Then, the composite solder was investigated under the 10^4 A/cm^2 of current density and 120 °C ambient temperature. For the comparative study, non-composite e-SAC solder was also investigated under the same experimental conditions. Three major conclusions were obtained through this study:

1. The Sn–Sb particles were formed in the solder matrix after the first-reflow. The average size of the Sn–Sb particles was 68.32 μm^2, and the area fraction of the Sn–Sb particles was reached to 11.14%. After 240 h of current stressing, the shape and size of Sn–Sb particles remained, but most of them broke and detached from the solder matrix due to its brittleness and immobility during the current stressing.
2. The directional movement of metal atoms/ions under high current density generated the compressive stress at the anode side. Both in composite eutectic SnAgCu solder and non-composite one, the compressive stress induced the bulge of solder and Sn–Cu IMCs after 240 h of current stressing.
3. Due to the ductility of e-SAC solder, there was more uniform plastic deformation at the cathode side due to the tensile stress induced by migration of the metal atoms/ions. However, in the composite one, the Sn–Sb particles at the edge blocked the movement of the solder atoms/ions that caused a current crowding region. As a result, the rapid increase of temperature melted down the solder at the edge where the crack was formed. Under the tensile stress at the cathode side, the crack propagated from the edge to the inner part of the interface. Thus, the ex-situ particles in solder matrix, especially the larger-size ones, could favor the current crowding and induce the ultimate failure of the joints at the cathode side.

Acknowledgements The authors acknowledge the financial support of this work from the Beijing Natural Science Foundation Program and Scientific Research Key Program of Beijing Municipal Commission of

Education (KZ200910005004), the Academic Innovation Group Supporting Program of Beijing Municipality, and the China Scholarship Council (2008654006). The authors also acknowledge the revision of manuscript from writing centre at Michigan State University.

References

1. Puttlitz KJ, Galyon GT (2007) J Mater Sci Mater Electron 18:331
2. Guo F, Lucas JP, Subramanian KN (2001) J Mater Sci Mater Electron 12:27
3. Guo F, Lee J, Choi S, Lucas JP, Bieler TR, Subramania KN (2001) J Electron Mater 30:1073
4. Hao H, Shi Y, Xia Z, Lei Y, Guo F (2008) J Electron Mater 37:2
5. Cheng F, Nishikawa H, Takemoto T (2008) J Mater Sci 43:3643. doi:10.1007/s10853-008-2580-7
6. Lin YC, Zhong J (2008) J Mater Sci 43:3072. doi:10.1007/s10853-007-2320-4
7. Wu BY, Chan YC, Zhong HW, Alam MO (2007) J Mater Sci 42:7415. doi:10.1007/s10853-007-1836-y
8. Nah JW, Suh JO, Tu KN, Yoon SW, Rao VS, Vaidyanathan K, Hua F (2006) J Appl Phys 100:1235131
9. Chen CM, Huang CC, Liao CN, Liou KM (2007) J Electron Mater 36:760
10. Chen CM, Huang CC (2008) J Alloys Compd 461:235
11. He HW, Xu GC, Guo F (2009) J Mater Sci 44:2089. doi:10.1007/s10853-009-3276-3
12. Xu GC, He HW, Guo F (2009) J Electron Mater 38:273
13. Xu GC, He HW, Guo F (2009) J Mater Sci Mater Electron 20:276
14. Lee HT, Lin HS, Lee CS, Chen PW (2005) Mater Sci Eng A 407:36
15. Ren F, Nah JW, Tu KN, Xiong BS, Xu LH, Pang J (2006) Appl Phys Lett 89:141914
16. Nah JW, Ren F, Paik KW, Tu KN (2006) J Mater Res 21:698
17. Chen C, Liang SW (2007) J Mater Sci Mater Electron 18:259